The Astrophysical Journal, 617:1191–1203, 2004 December 20

OPTICAL OUTFLOWS IN THE R CORONAE AUSTRALIS MOLECULAR CLOUD

Hongchi Wang,[1,2] Reinhard Mundt,[2] Thomas Henning,[2] and Dániel Apai [2]

Received 2004 June 4; accepted 2004 August 30

ABSTRACT

A deep [S II] $\lambda\lambda$6717/6731 wide-field survey of Herbig-Haro (HH) objects has been carried out in two fields toward the R CrA molecular cloud using the ESO/MPG 2.2 m Wide Field Imager. Twelve new HH objects, many of which consist of several condensations or knots, have been discovered, and new details of the known HH objects have been revealed. Combining the results of previous optical, infrared, and millimeter-wavelength observations, the possible exciting sources of HH objects in the region are discussed. On the basis of the previously known and newly discovered HH objects, at least five HH flows in the region around R CrA and at least two outflows in the region around VV CrA can be identified. In combination with the previously detected molecular outflows, the HH flows in the R CrA region indicate rather active star formation in the R CrA core in the past 10^5–10^6 yr.

Subject headings: ISM: Herbig-Haro objects — ISM: individual (R Coronae Australis IRS 7) — ISM: jets and outflows — stars: formation

1. INTRODUCTION

In the early phase of star formation, mass outflows are believed to be driven by young stars along their polar axes even though they are still at the stage of mass accretion from their environments (e.g., Shu et al. 1994). Herbig-Haro (HH) objects and HH jets, a kind of nebulae with characteristic shock-excited emission lines (Schwartz 1978), are an important tracer of the high-velocity ($\sim$100–400 km s^{-1}) matter ejected from young stars. This highly supersonic gas is interacting with the surrounding medium or with slower gas ejected during previous outflow phases, giving rise to a broad variety of shock-excited emission-line nebulae, both in morphology and excitation. Because of their relatively short dynamical ages, HH objects trace recent star formation in molecular clouds and can in principle provide unique information on the exciting sources, such as the accretion history (for reviews, see, e.g., Eislöffel et al. 2000; Reipurth & Bally 2001). Unfortunately, such a relatively small molecular cloud as the R CrA cloud is not well suited to trace the outflow activity very long into the past, because the crossing time for an outflow from the center to the edge of the cloud is only 1500 yr (for an outflow velocity of 200 km s^{-1} and $r_{\rm cloud} = 0.3$ pc). Nevertheless, a survey of the cloud will trace the recent star formation activity in R CrA. Taking advantage of the large field of view as well as the high resolution and sensitivity provided by large format CCD detectors, optical emission line surveys can provide unique information on the star formation activity in an entire cloud.

The Corona Australis molecular cloud, at a distance of 170 pc (Knude & Høg 1998), is one of the nearest star-forming regions. Molecular line mapping revealed a cometary-shaped cloud complex oriented in the northwest-southeast direction (Loren 1979; Harju et al. 1993; Yonekura et al. 1999). The cloud complex is dominated by a dense core at the cometary head, the so-called R CrA core, which is $11' \times 20'$ in extent and contains a mass of about 50 $M_\odot$ (Harju et al. 1993). Among the most massive stars in that core are TY CrA (B9) and R CrA (A5e) (Herbig & Bell 1988). Both stars are associated with bright reflection nebulae and are typical members of the class of Herbig Ae/Be stars. Surveys in Hα (e.g., Knacke et al. 1973; Marraco & Rydgren 1981) and X-ray emission (e.g., Neuhäuser et al. 2000) revealed a population of low-mass young stars around R CrA. Near-infrared observations found an embedded association, which is named the "Coronet" (Taylor & Storey 1984). Deep near-infrared imaging by Wilking et al. (1997) led to the discovery of additional young stars in the cloud. Deeply embedded sources were detected by centimeter (Brown 1987; Suters et al. 1996) and millimeter continuum observations (Reipurth et al. 1993; Henning et al. 1994; Chini et al. 2003; Choi & Tatematsu 2004). One molecular outflow (Anderson et al. 1997) and eight HH objects, HH 82, 96–101, and 104, have been found in the region (Strom et al. 1974; Cohen et al. 1984; Schwartz et al. 1984; Hartigan & Graham 1987; Reipurth & Graham 1988; Graham 1993). However, the previous HH object observations had either small sky coverage ($\lesssim 11' \times 11'$; see, e.g., Reipurth & Graham 1988; Graham 1993) or low sensitivity (see, e.g., Strom et al. 1974; Cohen et al. 1984; Schwartz et al. 1984). In this paper we report the results of a deep and wide-field [S II] $\lambda\lambda$6717/6731 survey of HH objects in the R CrA cloud.

2. OBSERVATIONS AND DATA REDUCTION

The observations were made during 2002 September 1–3 using the ESO/MPG 2.2 m telescope at La Silla. The telescope is equipped with the Wide Field Imager (WFI) camera, which is a mosaic of eight 2K $\times$ 4K CCDs with narrow interchip gaps (the filling factor is 95.9%) (Baade 2002). With a plate scale of $0\farcs238$ pixel^{-1}, the total field of view of WFI is $34' \times 33'$. The combination of the filters ESO 857 and ESO 847 was used for the observations. The ESO 857 filter is a narrowband filter with a central wavelength of $\lambda_c = 6763.4$ Å and a bandpass of $\Delta\lambda = 84.2$ Å. Its transmission at the characteristic lines of HH objects, [S II] $\lambda\lambda$6717/6731, is 0.31 and 0.63, respectively. The ESO 847 filter, an intermediate-band filter with a central wavelength of $\lambda_c = 7217.9$ Å and a bandpass of $\Delta\lambda = 256.5$ Å, was used to measure the continuum emission. The details on these filters can be found on the ESO Web site.[3] Unfortunately, there are

[1] Purple Mountain Observatory, Academia Sinica, Nanjing 210008, China; hcwang@pmo.ac.cn.

[2] Max-Planck-Institut für Astronomie, Königstuhl 17, D-69117 Heidelberg, Germany.

[3] See http://www.ls.eso.org/lasilla/sciops/2p2/E2p2M/WFI/filters.

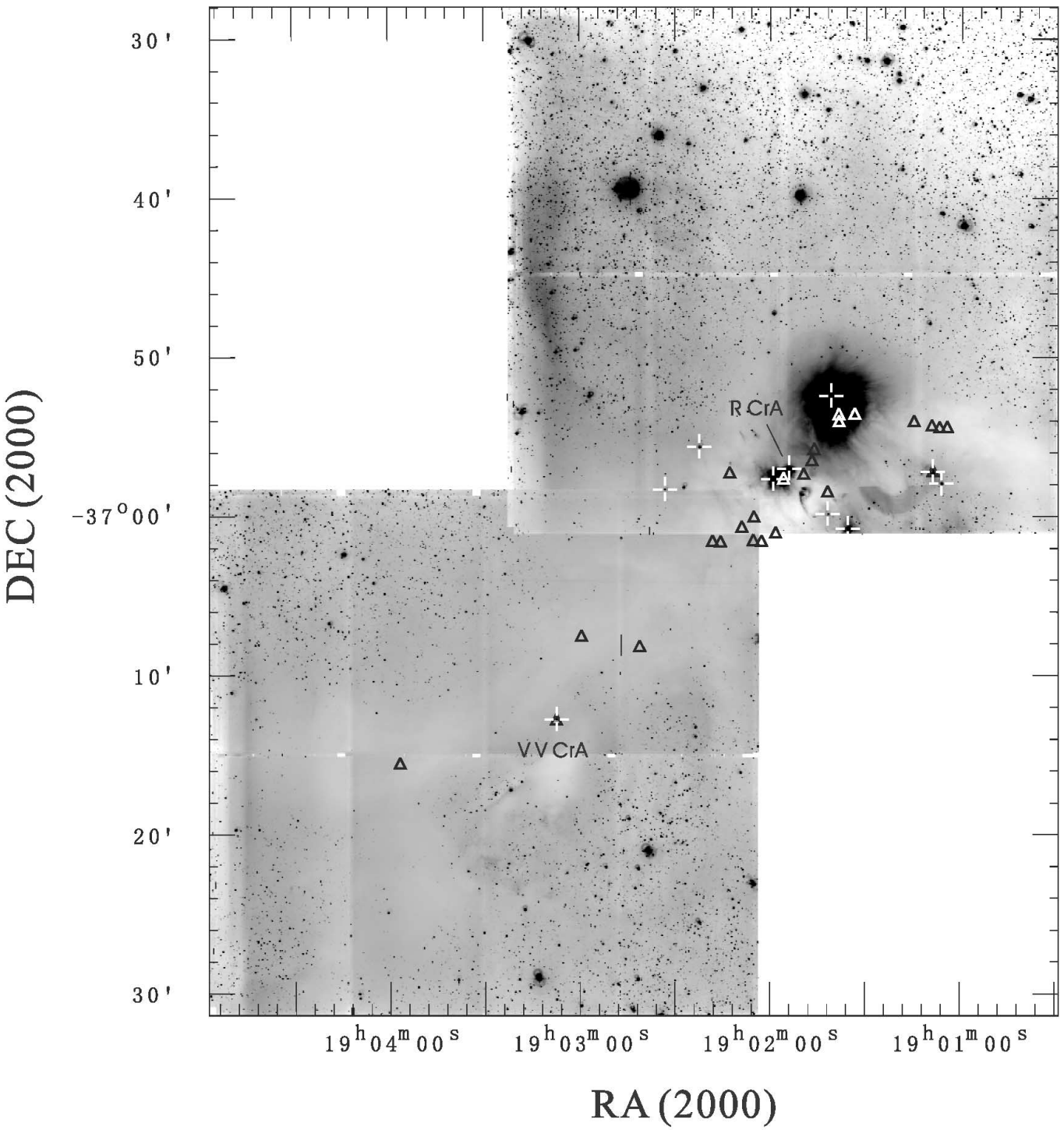

FIG. 1.—[S II] image of the R CrA cloud. The known Hα emission stars in the region (Herbig & Bell 1988) are marked with white plus signs. The stars R CrA and VV CrA are indicated for orientation. The known millimeter sources from Chini et al. (2003) are marked with triangles. The small white rectangles in the middle of each field are the interchip areas that were not covered by any CCD chip because of the imperfect dithering scheme used in the observations.

ringlike artifacts around bright stars. These artifacts are due to the internal reflections of stars, which can happen at different levels, for instance, between the lenses of the corrector, between the lenses and the filter, or between the filter and the CCD window. These artifacts are marked by "AR" in the displayed images.

Two fields toward the R CrA cloud were observed during our survey (see Fig. 1). To eliminate the effects of interchip gaps, cosmic rays, and bad pixels, six frames were taken in each of the ESO 857 and ESO 847 filters with the telescope pointing being slightly offset. However, in our images there are still four small areas ($\sim 28'' \times 14''$) in each field that were not covered by any CCD chip because of the imperfect dithering scheme used in the observations (Fig. 1, *small white rectangles*). The total exposure times for each field in the ESO 857 ([S II]) and ESO 847 (continuum) filters were 150 and 48 minutes, respectively. The seeing during the observations was around $0\farcs9$.

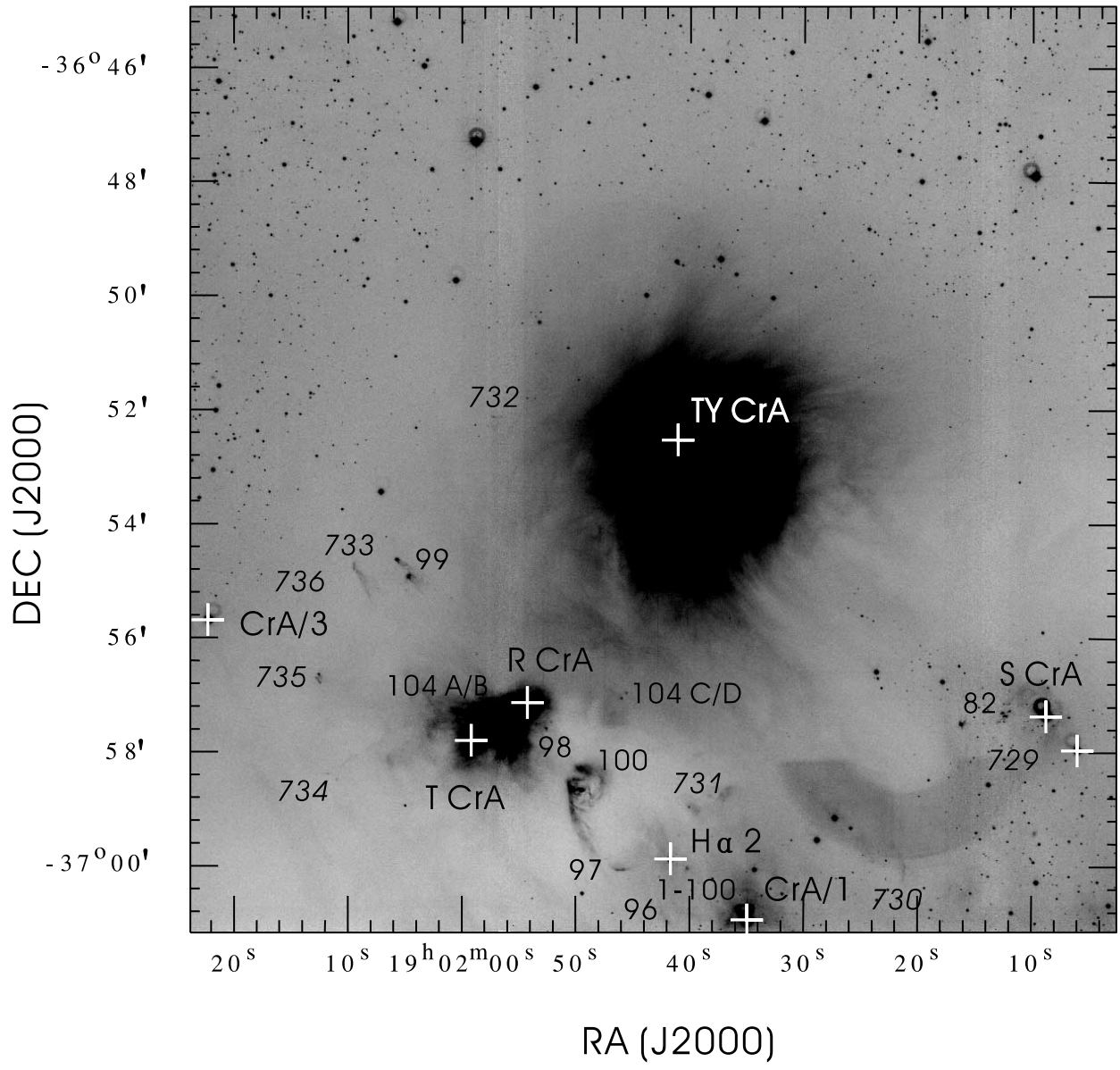

FIG. 2.—[S II] image of the R CrA region. The Hα emission stars in the region (Herbig & Bell 1988) are marked with white plus signs. Known (HH 82, 96–100, 104, and 1-100) as well as new (HH 729–736, in italics) HH objects are indicated.

Data reduction was made by using the MSCRED package in IRAF.[4] The frames were first bias-subtracted and dome flat field divided. Then the individual frames were registered and image distortion corrected. All frames for the same field and in the same filter were combined. In order to determine the flux ratios of stars between the ESO 847 and ESO 857 images, around 70 stars in each field were selected. The fluxes of these stars were measured using aperture photometry. Finally, a brightness scaled and positionally aligned ESO 847 image was subtracted from the ESO 857 image. The resulting image was visually examined to identify all HH objects in the region.

3. RESULTS

Our survey covered two fields of the R CrA cloud. These fields, each with a field of view of $\sim 34' \times 33'$, are shown in Figure 1. The emission-line stars in the region found in several Hα emission surveys (Herbig & Bell 1988) are marked with white plus signs.

All of the previously known HH objects in the region, HH 82, 96–100, and 104 (Strom et al. 1974; Cohen et al. 1984; Schwartz et al. 1984; Hartigan & Graham 1987; Reipurth & Graham 1988; Graham 1993), are detected in our survey. We emphasize that our imaging of the region is much deeper and has a higher spatial resolution than previous observations. Additionally, our survey has much larger sky coverage. As a result of these advantages, 12 new HH objects are discovered in our survey. In addition, two HH knots, designated HH 98B and 99C, are discovered in the vicinity of HH 98 and 99, respectively.

The newly found HH objects are concentrated in regions around R CrA and VV CrA. The [S II] images of these regions are shown in Figures 2 and 7*a*. After the subtraction of the continuum emission, HH objects can be more easily identified, as shown in Figures 3–6 and in Figures 7*b*–7*d*. Table 1 lists the coordinates of the newly detected HH objects and gives a short

[4] IRAF is distributed by the National Optical Astronomy Observatory, which is operated by the Association of Universities for Research in Astronomy, Inc., under cooperative agreement with the National Science Foundation.

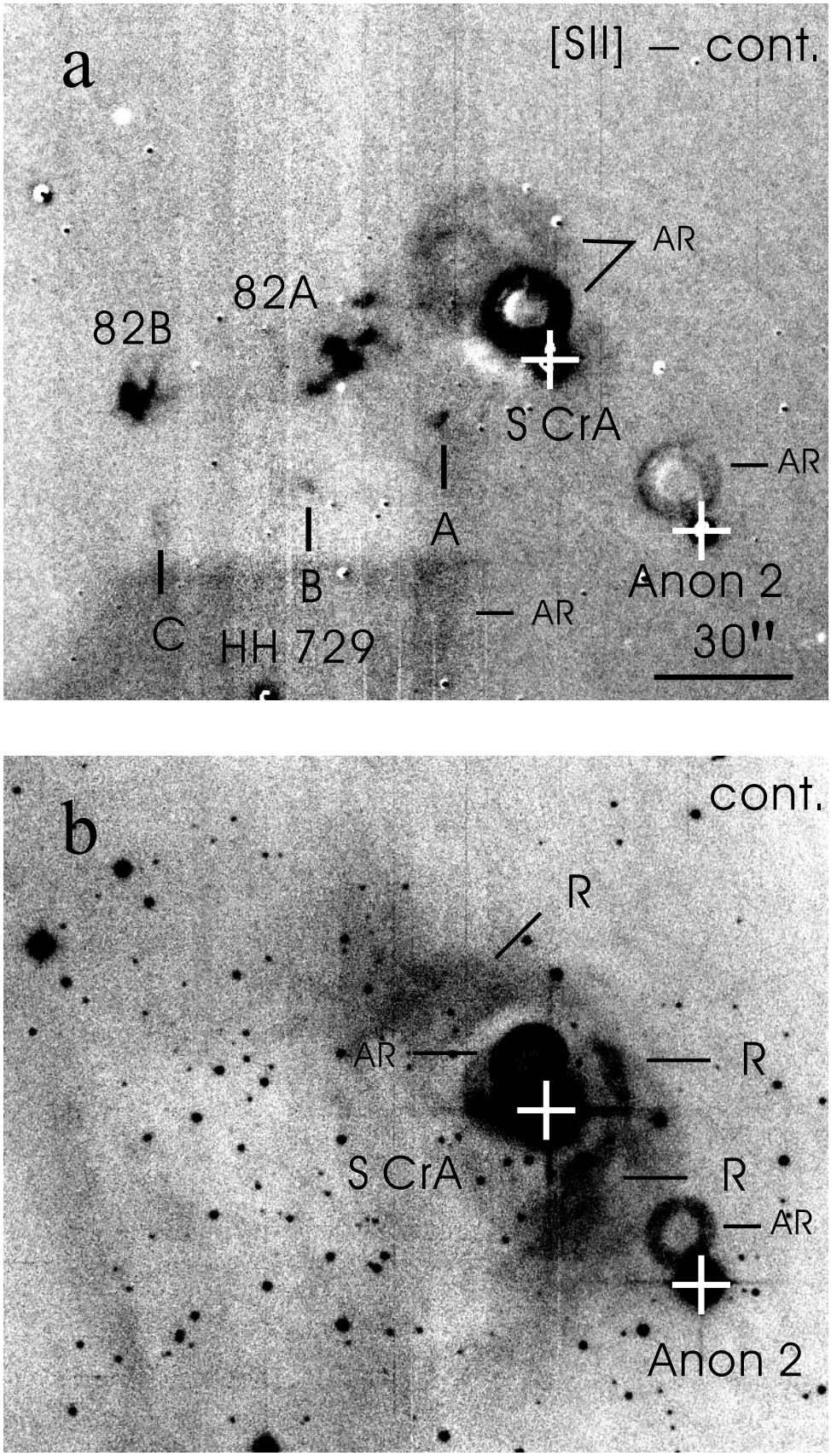

FIG. 3.—(*a*) Continuum-subtracted [S II] and (*b*) continuum images of the S CrA region. HH 729 A–C, together with the previously known objects HH 82 A and B, are marked in (*a*). The arclike reflection nebula surrounding S CrA visible in the continuum image is indicated with R. Artifacts in the images are indicated with AR. North is up, and east is to the left.

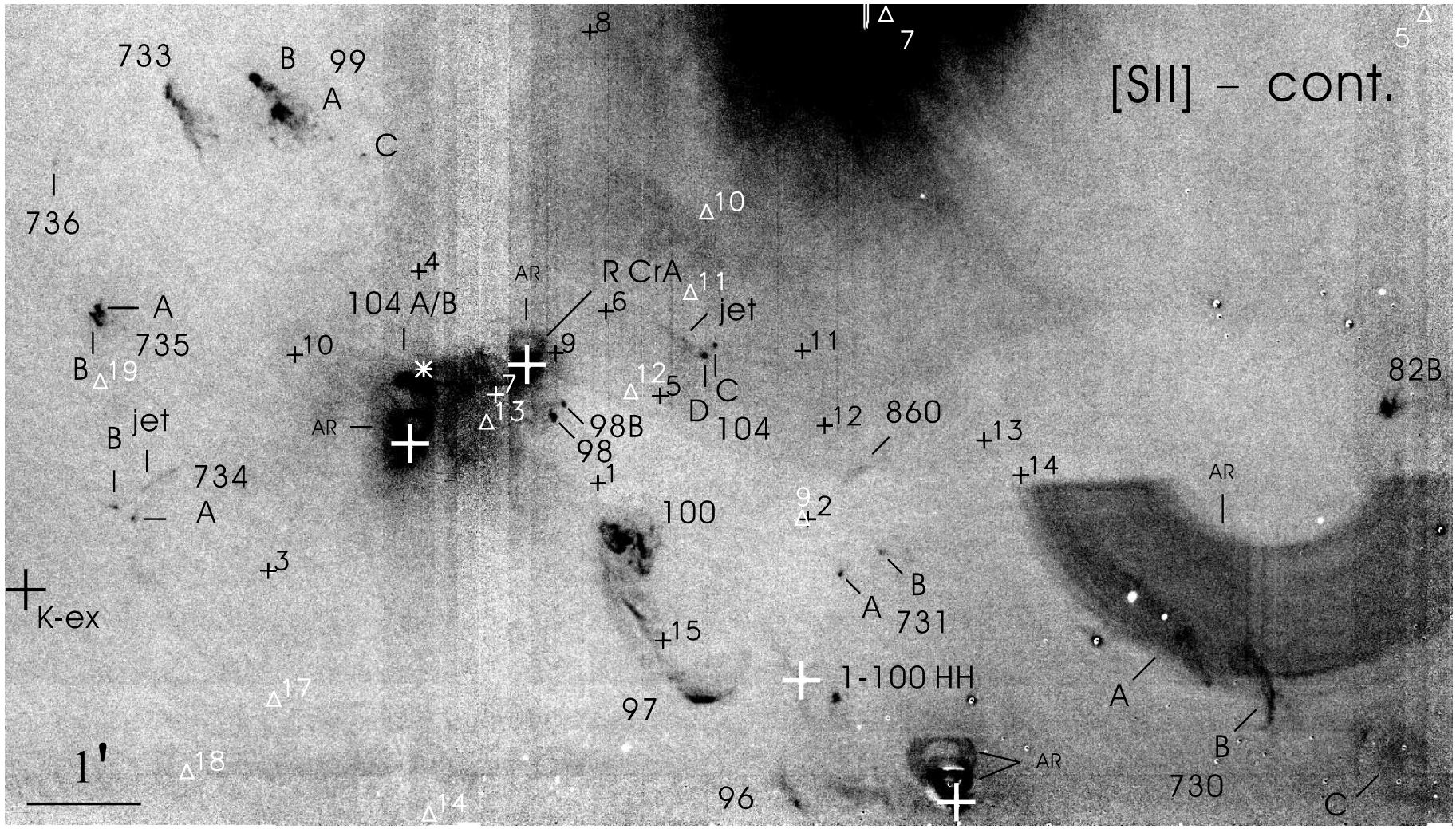

FIG. 4.—Continuum-subtracted [S II] emission of the R CrA region. The previously known and newly discovered HH objects are indicated. The Hα emission stars in the Herbig & Bell (1988) catalog (*right to left*, CrA/1, Hα 2/star 1-100, R CrA, and T CrA) are marked with large white plus signs. The infrared sources detected by Taylor & Storey (1984) are marked with small plus signs and labeled. The millimeter sources from Chini et al. (2003) are marked with white triangles. The embedded star WMB 55 (Gezari et al. 1999) is marked with an asterisk. The *K*-excess star ($\alpha = 18^{\rm h}58^{\rm m}53\overset{\rm s}{.}3$, $\delta = -37^{\circ}03'28''$ [B1950.0]; Wilking et al. 1997) is marked with a large black plus sign. Artifacts are marked with AR. North is up, and east is to the left.

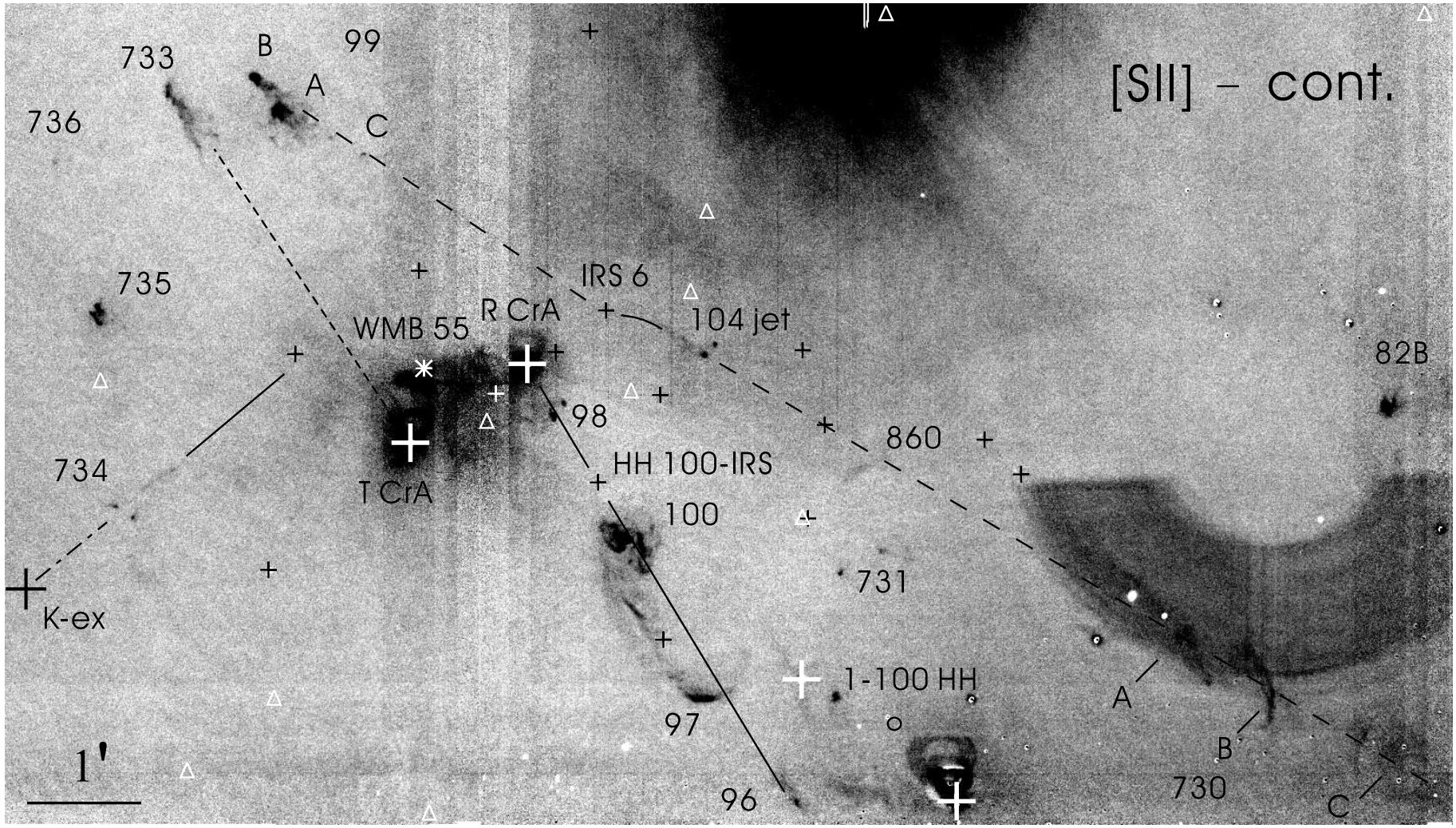

FIG. 5.—Possible optical outflows identified in the R CrA region on the basis of the morphology. As discussed in the text, the verification of the suggested outflow sources requires proper-motion and radial velocity measurements.

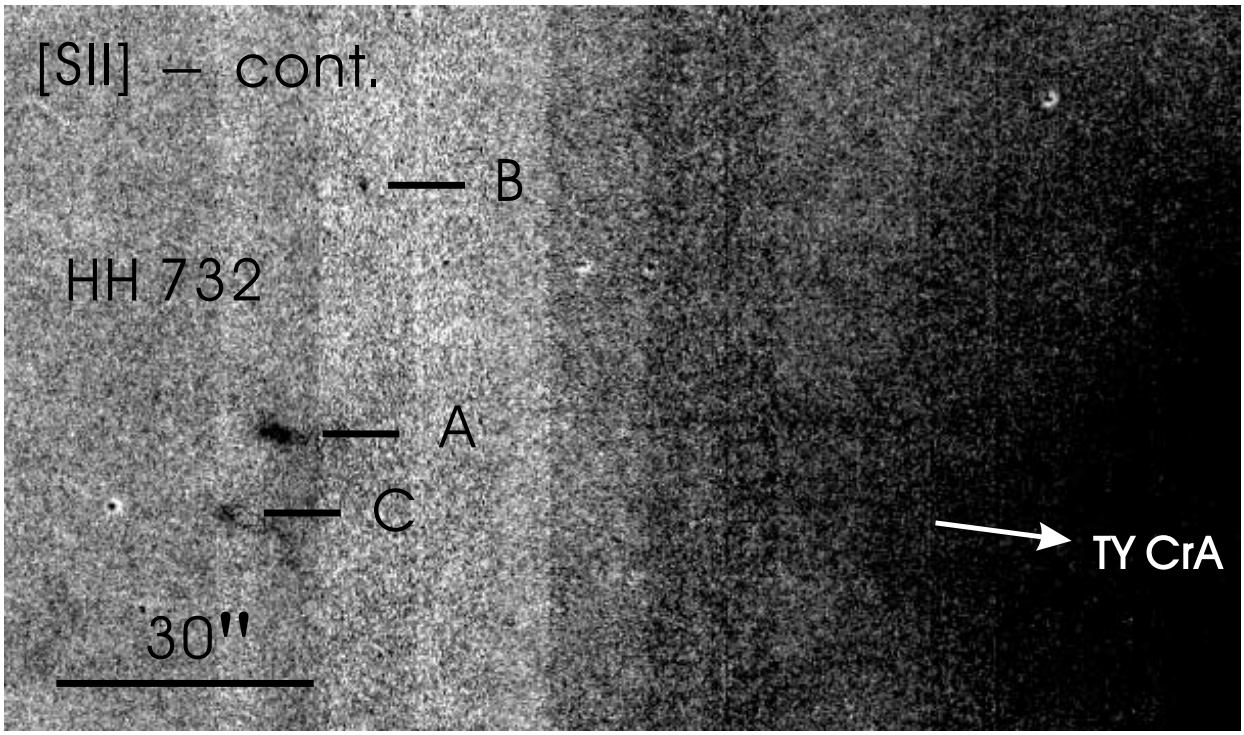

FIG. 6.—Continuum-subtracted [S II] image of the newly detected HH object HH 732. North is up, and east is to the left.

description of their morphology. Many of these new HH objects consist of several condensations or knots or other substructure. Except for HH 860–863, which are diffuse, the coordinates in Table 1 refer to positions of the maximum [S II] emission. For HH 860–863, which are diffuse patches, their position averages are given in Table 1. To show the details and to be more specific about the coordinates given in this paper, [S II] emission contours of all the complex HH objects in the region, including the known HH objects, are given in Figure 8. To estimate the accuracy of our astrometry, we compared the coordinates of stars measured from our [S II] image with those compiled in the USNO2 catalog. It was found that our astrometry is accurate within 0.″3 both in right ascension and declination.

All known HH objects in the region have coordinates determined at an epoch before 1992. However, most of these coordinates were determined with Schmidt plates and usually have a large uncertainty. Furthermore, the coordinates might just be position averages over the HH objects, rather than referring to any specific spot, such as the emission maxima. This situation prevents us from estimating proper motions for the known HH objects. To facilitate a future estimation of proper motions of HH objects in the R CrA cloud, the coordinates of the known HH objects measured from our [S II] images are given in Table 2. These coordinates refer to the [S II] emission maxima (see Fig. 8).

4. NOTES AND DISCUSSION OF INDIVIDUAL HH OBJECTS

In the following discussion we try to identify the exciting sources of the individual HH objects. Unfortunately, in most cases we have no proper-motion and radial velocity measurements available, and therefore we base this part of the discussion on the orientation and alignment of HH objects with potential driving sources.

4.1. *Region around R CrA*

4.1.1. *HH 82 and 729 near S CrA*

HH 82A and 82B are two bright HH objects located to the east of the well-known T Tauri star S CrA (e.g., Appenzeller & Wolf 1977; Mundt 1979; see our Fig. 3). S CrA coincides well with the millimeter source MMS 1 (Chini et al. 2003). On the basis of their vicinity to and their alignment with S CrA, Reipurth & Graham (1988) proposed that these HH objects are driven by S CrA. This suggestion is plausible, since S CrA shows various signs of a strong mass outflow. These signs are blueshifted absorption features in the Na D and Ca II H and K lines (e.g., Mundt 1984; Appenzeller et al. 1986) and highly blueshifted forbidden emission lines (e.g., Appenzeller et al. 1984). T Tauri stars with such spectroscopic signatures of outflows are frequently HH object sources (e.g., Mundt & Eislöffel 1998). Furthermore, an arclike reflection nebula surrounds S CrA (see Fig. 3*b*). This reflection nebula is open in the direction toward HH 82, supporting that the HH 82 flow is driven by S CrA. We note that for several other HH object sources a similar morphology is observed. Somewhat puzzling are the additional HH objects HH 729 A–C, located roughly 30″ south of HH 82. The knots 729 A–C line up very well with S CrA, and therefore it is rather suggestive that they are also driven by S CrA.

Why are there apparently two independent flows driven by S CrA? Two explanations are possible: (1) each of these two flows might be driven by a different member of the S CrA binary system (separation = 1″ by Joy & van Biesbroeck 1944 and separation = 1.″4 by Ghez et al. 1997); (2) the brighter component of the S CrA system, which clearly shows spectroscopic signs for strong mass loss, created a poorly collimated ovoid-shaped outflow cavity, and HH 82 and HH 729 trace more or less the edge of this cavity. Several other examples are known

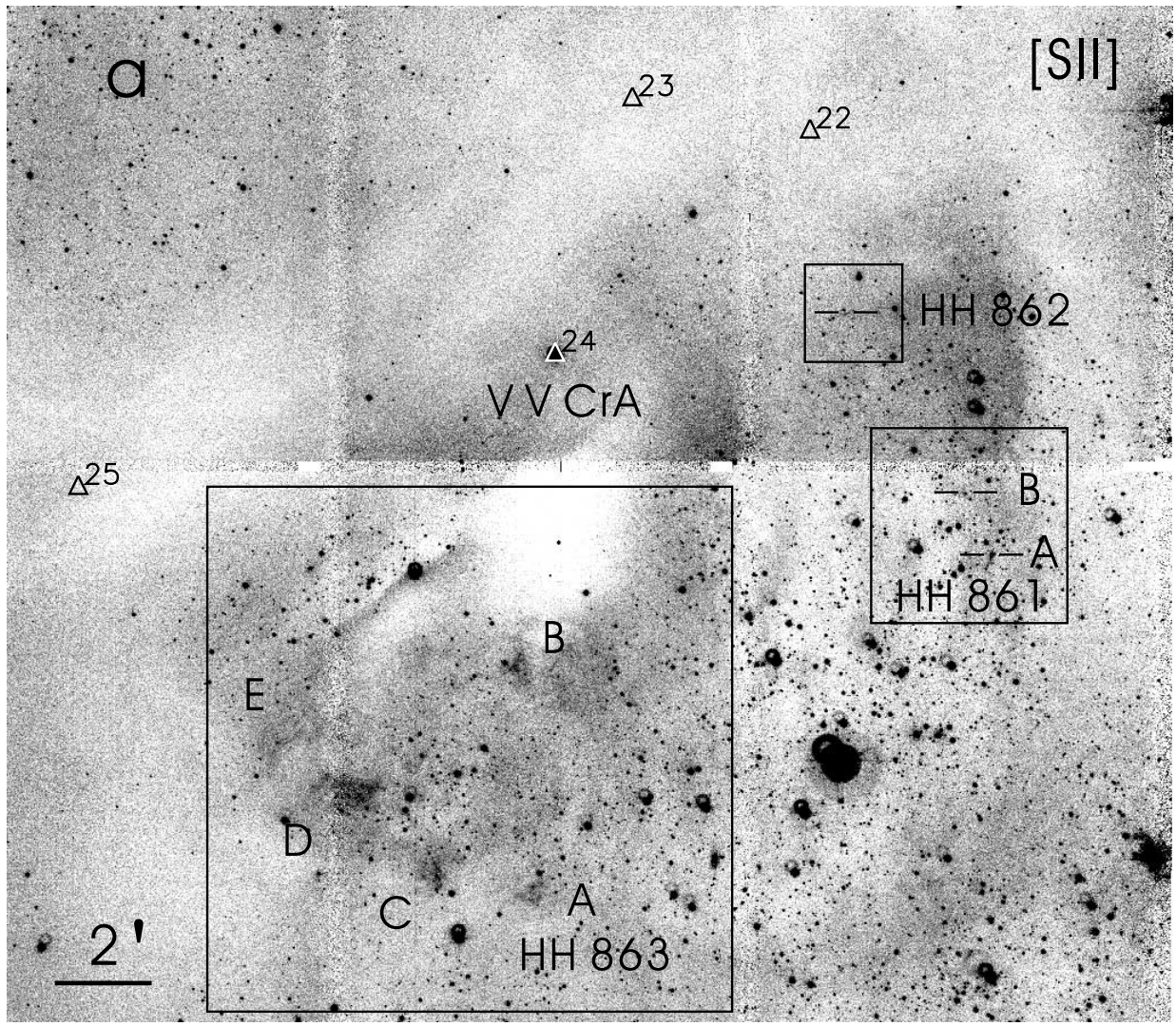

FIG. 7.—[S II] image of (*a*) the VV CrA region and (*b–d*) the continuum-subtracted [S II] images of the newly discovered HH objects. The millimeter sources in the region from Chini et al. (2003) are marked with triangles. North is up, and east is to the left.

TABLE 1
NEWLY DISCOVERED HERBIG-HARO OBJECTS IN R CrA

Object	α (J2000.0)	δ (J2000.0)	Comments
HH 729A	19 01 10.56	−36 57 32.4	Patch
HH 729B	19 01 12.94	−36 57 48.2	Faint patch
HH 729C	19 01 15.68	−36 57 56.4	Faint patch
HH 730A	19 01 25.26	−36 59 30.0	Curved line
HH 730B	19 01 24.08	−36 59 59.8	Arc
HH 730C	19 01 15.72	−37 00 30.0	Complex of diffuse patches
HH 860	19 01 39.40	−36 58 03.8	Patch
HH 731A	19 01 40.03	−36 58 57.3	Bright knot
HH 731B	19 01 38.27	−36 58 45.6	Knot with an extension
HH 98B	19 01 52.15	−36 57 28.4	Knot
HH 732A	19 01 57.20	−36 52 07.2	Elongated knot
HH 732B	19 01 56.41	−36 51 38.4	Knot
HH 732C	19 01 57.73	−36 52 17.0	Faint patch
HH 99C	19 02 00.91	−36 55 17.5	Knot
HH 733	19 02 09.47	−36 54 46.2	Bright patch with a tail
HH 734A	19 02 11.01	−36 58 28.6	Knot
HH 734B	19 02 11.73	−36 58 22.7	Curved jet
HH 735A	19 02 12.56	−36 56 37.8	Bright elongated knot
HH 735B	19 02 12.76	−36 56 42.1	Bright elongated knot
HH 736	19 02 14.41	−36 55 22.2	Faint patch
HH 861A	19 02 21.57	−37 16 55.0	Faint patch
HH 861B	19 02 24.30	−37 15 38.0	Patch
HH 862	19 02 36.58	−37 11 57.2	Elongated patch
HH 863A	19 03 09.01	−37 23 55.7	Faint patch
HH 863B	19 03 10.82	−37 19 12.3	Patch
HH 863C	19 03 18.60	−37 23 31.2	Faint patch
HH 863D	19 03 26.91	−37 21 54.4	Patch
HH 863E	19 03 31.70	−37 20 32.6	Faint patch

NOTE.—Units of right ascension are hours, minutes, and seconds, and units of declination are degrees, arcminutes, and arcseconds.

(e.g., Haro 6-5B and L1551 IRS 5) where the edges or other parts of an ovoid-shaped wind-blown cavity are traced by HH objects (see Eislöffel & Mundt 1998 for a discussion of related examples). If HH 82 and 729 are indeed driven by different members of the S CrA binary system, then the long-slit spectroscopic observations by Takami et al. (2003) suggest that the brighter component A probably excites HH 729, because the [S II] emission of S CrA measured by Takami et al. (2003) is displaced toward position angle (P.A.) $\sim 147^\circ$. This P.A. is much closer to the P.A. of the HH 729 flow (P.A. $\sim 115^\circ$) than the HH 82 flow (P.A. $\sim 95^\circ$), and therefore it is relatively unlikely that HH 82 is excited by the brighter component.

4.1.2. *HH 730, 860, 104 C–D, and 99: A Possible Giant Outflow Driven by IRS 6*

In the R CrA region a possible giant outflow is identified on the basis of the previously known HH objects HH 99 and the newly discovered HH objects HH 730, 860, and the 104 D jet (see Figs. 4 and 5). This giant flow is 0.57 pc in extent ($\sim 12'$) at the distance of the R CrA cloud. The exciting source of this outflow is apparently the nebulous IR source IRS 6 found by Wilking et al. (1997). These authors found by H_2 imaging a curved jet extending from IRS 6 toward the southwest. The southwestern end of this H_2 jet coincides with the optical jet associated with HH 104D. The curving of the southwestern outflow from IRS 6 can explain why the optical jet associated with HH 104D does not point toward IRS 6. The southwestern part of this outflow is furthermore traced by the newly discovered HH objects HH 860 and HH 730 A–C. The relatively diffuse emission from HH 730 A–C are evident in Figs. 4 and 5, although they are superposed on a large and diffuse ghost image of TY CrA. HH 730A is a curved line, and HH 730B is a large arc. HH 730C is a complex of diffuse patches.

The opposite side (i.e., the northeastern side) of this giant outflow is traced only by HH 99 A–C. In the H_2 images of Wilking et al. (1997) a nice bow shock can be seen at the position of HH 99 B, with the axis pointing toward IRS 6. The bow shock structure of HH 99 is not obvious in our optical images. However, our observations reveal more details of HH 99A and 99B than previous optical studies. Both HH 99A and 99B show a bright compact head and a faint diffuse tail. A bright knot, designated HH 99C, and several faint knots can be identified to the southwest and south of HH 99A.

As already mentioned above, the IR images of Wilking et al. (1997) show that IRS 6 is associated with a reflection nebula and an emission-line jet. Therefore, this IR source has the clear characteristics of a young outflow source and cannot be a background star. From the IR colors published by Wilking et al. (1997) it is not clear, however, whether this star has indeed a strong IR excess or whether it could be only a highly reddened T Tauri star with the rather red IR colors mostly resulting from intercloud reddening (see their Fig. 6). Since there could be considerable variations in the intercloud reddening vector from source to source, it will not be possible to disentangle in individual cases intrinsic IR excess from intercloud reddening.

The source IRS 12 found by Taylor & Storey (1984) is located on the axis of the giant outflow apparently driven by IRS 6 and might therefore be considered an alternative driving source. However, this source was detected neither by Wilking et al. (1997) nor by 2MASS and might therefore not be a real source.

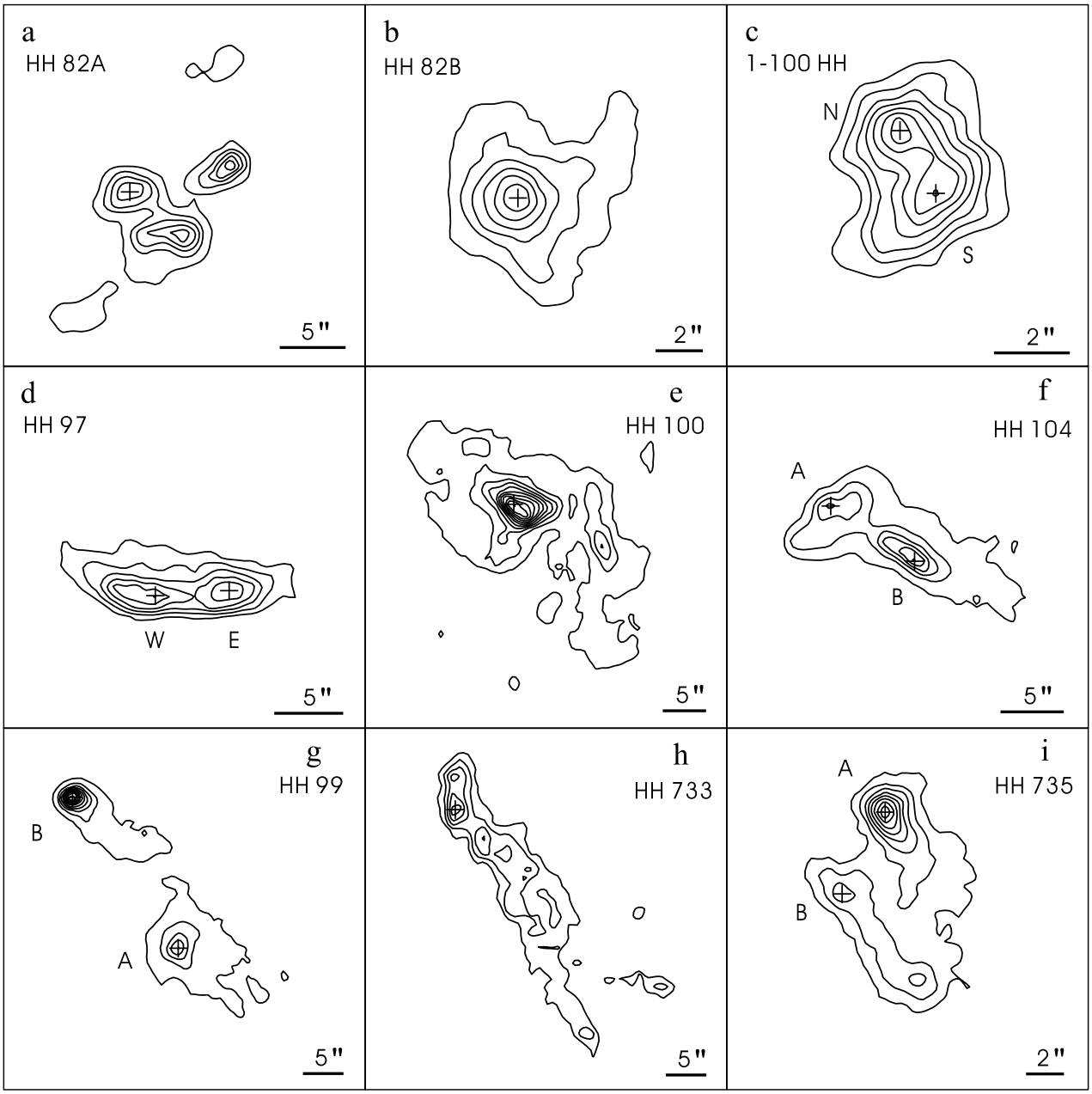

FIG. 8.—[S II] emission contours of HH 82A, 82B, 1-100HH, 97, 100, 104A/B, 99, 733, and 735. The lowest contours in panels (*a*)–(*i*) are, respectively, 5, 5, 5, 5, 5, 3, 5, 2, and 5 times the local background noise. The contour steps are, respectively, 5, 7, 2, 3, 6, 5, 12, 2, and 5 times the local background noise. The positions corresponding to the coordinates in Tables 1 and 2 are indicated with plus signs.

We finally note that the sources IRS 13 and 14 located west of HH 860 are unlikely HH object sources, because they are not associated with any IR reflection nebulosity and their IR colors are consistent with reddened background stars.

4.1.3. *HH 96, 97, 100, and 98*

Four HH objects, i.e., HH 96–98 (Hartigan & Graham 1987) and 100 (Strom et al. 1974), have been previously found to the southwest of R CrA. More details of these known HH objects are revealed in our continuum-subtracted [S II] image shown in Figure 4. HH 97 and 100 have complex structures (see Fig. 4 and Figs. 8*d* and 8*e*). HH 97 consists of two condensations of nearly equal brightness, 97W and 97E (Fig. 8*d*). A considerable morphology change of HH 100 during the time from 1973 to 1983 has been noted by Graham (1993). We detected a new HH knot, designated 98B, to the northwest of HH 98 (Fig. 4).

On the basis of alignment, it has been proposed that HH 101 (outside of our survey area), 96, 97, 100, 98, and 99 are part of a flow driven by the infrared source IRS 1/HH 100-IRS (Strom et al. 1974; Cohen et al. 1984; Schwartz et al. 1984; Hartigan & Graham 1987). As we discussed in § 4.1.2, HH 99 is most probably part of another flow in the region; therefore, it has no connection with HH 96–98 and 100. In Figure 5, the flow consisting of HH 96, 97, 100, and 98 is indicated with a solid line. A likely source of this flow is IRS 1/HH 100-IRS, a Class I source (Wilking et al. 1986, 1992). The arrangement of HH 96, 97, 100, and 98 does not exclude R CrA as the driving source. Radial velocity measurements have shown that HH 96 ($v \sim -52$ km

TABLE 2
KNOWN HH OBJECTS IN R CrA

Object	α (J2000.0)	δ (J2000.0)	Comments
82A	19 01 12.48	−36 57 17.5	Bright arclike knot
82B	19 01 16.09	−36 57 29.3	Complex of bright knots
1-100 HH N	19 01 40.19	−37 00 01.1	Northern condensation
1-100 HH S	19 01 40.11	−37 00 02.5	Southern condensation
96	19 01 41.87	−37 00 57.3	Patch
97W	19 01 45.75	−37 00 02.9	Western condensation
97E	19 01 46.20	−37 00 03.9	Eastern condensation
100	19 01 49.51	−36 58 39.7	Complex of patches
98	19 01 52.49	−36 57 34.9	Arclike knot
104A	19 01 59.24	−36 57 14.8	Bright patch
104B	19 01 58.68	−36 57 18.8	Bright patch
104C	19 01 45.46	−36 56 57.1	Knot
104D	19 01 45.91	−36 57 03.1	Highly collimated jet
99A	19 02 04.63	−36 54 55.7	Bright knot with a tail
99B	19 02 05.72	−36 54 37.2	Bright knot with a tail

NOTE.—Units of right ascension are hours, minutes, and seconds, and units of declination are degrees, arcminutes, and arcseconds.

s^{-1}), 97 ($v \sim -125$ km s^{-1}), and 100 ($v \sim -133$ km s^{-1}) are blueshifted, while HH 98 ($v \sim +3$ km s^{-1}) is slightly redshifted (Strom et al. 1974; Hartigan & Graham 1987). The radial velocity of HH 98 is surprisingly small, if this HH object traces the counterflow to HH 96, 97, and 100, and if all these HH objects are driven by IRS 1/HH 100-IRS. Proper-motion measurements are necessary to clarify the situation.

4.1.4. *HH 733*

HH 733 is 46″ east of HH 99B (Fig. 4). It has a bright head and a long, wide tail. Near-infrared H_2 emission has been detected at the head of HH 733 (Wilking et al. 1997; Davis et al. 1999). The morphology suggests that HH 733 and HH 99 represent different flows. We suggest that HH 733 is probably driven by the T Tauri star T CrA (Herbig & Bell 1988). This flow is indicated with a dotted line in Figure 5. On the other hand, it cannot be excluded that this outflow is driven by the deeply embedded source WMB 55, about which we give more details in § 4.1.5.

4.1.5. *HH 734*

HH 734 is located ∼2.′5 east of T CrA. HH 734A is a knot, while HH 734B is part of a curved jet. A near-infrared source showing clear excess emission in the K band ($\alpha = 18^h58^m53^s.3$, $\delta = -37°03'28''$ [B1950.0]; see Wilking et al. 1997) is located 64″ to the southeast of HH 734, nearly on the axis of the jet. Therefore, this star is a good candidate for the driving source of HH 734. This outflow is shown with a dot-dashed line in Figure 5. IRS 10 and 4 are located near the axis of the HH 734B jet, but their IR colors show that they are reddened background stars and therefore unlikely to be the driving source of HH 734.

Another possible driving source of HH 734 is WMB 55 (Gezari et al. 1999), which is located slightly offset from the axis of the jet. WMB 55 was detected in the H and K' bands, but not in the J band in the near-infrared imaging by Wilking et al. (1997). This star coincides well with the SCUBA 450 and 850 μm point-like source 6 (van den Ancker 1999) and also coincides with a 1.2 mm emission protuberance (see Fig. 3 of Chini et al. 2003). Therefore, WMB 55 seems to be a deeply embedded protostar. Although WMB 55 is offset from the axis of the HH 734B jet, it cannot be totally excluded as the exciting source of HH 734, considering the curved appearance of the HH 734B jet.

4.1.6. *HH 735 and 736*

About 2′ to the north of HH 734 lies the newly detected HH object HH 735 (Fig. 4). It consists of two bright knots, HH 735A and 735B. The images of these knots are very sharp edged. They are elongated in nearly parallel directions along a line running from northeast to southwest. HH 736 is a faint patch and is located about 1.′3 to the north of HH 735. Anderson et al. (1997) detected a millimeter outflow from IRS 7 at the direction of P.A. $\sim 75°$. The blueshifted lobe of this millimeter outflow coincides with HH 104 A/B. Indeed, radial velocity measurements show that both HH 104A ($v = -46$ km s^{-1}) and 104B ($v = -56$ km s^{-1}) are blueshifted (Hartigan & Graham 1987). HH 735 and 736 are located in the direction of the blueshifted lobe of the millimeter outflow. They probably trace the outer part of this blueshifted lobe and therefore are excited by IRS 7. It is also possible that HH 98 is the counterflow of HH 104 A/B on the basis of its location and its redshifted radial velocity.

Other possible sources for HH 735 are MMS 19 of Chini et al. (2003) and the Class I young stellar object (YSO) IRS 3 (Wilking et al. 1986, 1992). If one of these two sources is indeed exciting HH 735, they may also be the exciting source of HH 736, because it is roughly located along the lines connecting HH 735 with IRS 3 and MMS 19. We note that CrA/3 (Walter 1986; Herbig & Bell 1988), which is located about 1.′7 east of HH 736, is an unlikely outflow source because it is a weak-line T Tauri star.

On the basis of alignment, Graham (1993) suggested that HH 104 C/D are the counterflow of HH 104 A/B and that HH 104 A–D are driven by the young star R CrA. Our detection of the HH 104 D jet, which is oriented in the northeast-southwest direction, clearly rules out that HH 104 D has a physical association with HH 104 A/B and R CrA. In light of the close association of HH 104 C with 104 D, it is also unlikely that HH 104 C has a physical association with HH 104 A/B and R CrA.

A precessing outflow model was proposed by Anderson et al. (1997) to interpret the misalignment among HH 99 A/B, 101 N/S, 104 A/B, and the millimeter outflow. In this figure, the millimeter outflow and HH 104 A/B represent a younger generation of the bipolar outflow from IRS 7, while HH 99 A/B and 101 N/S represent an older generation. This figure, however, is not favored by our optical observations. First, as discussed in previous subsections, outflows in the R CrA region cannot be attributed to just one driving source. Second, we detected HH 735 and 736 along the blueshifted lobe of the millimeter outflow. Assuming that these HH objects trace the outer part of the millimeter outflow and that they have the same spatial velocity as HH 104 A/B, the dynamical age of the outflow in the direction of P.A. $\sim 75°$ is in fact similar to, rather than much younger than, that of the outflow in the northeast-southwest direction. A configuration of two outflows with orientation difference as large as 30° but of similar ages can hardly be explained by ejection axis precession of outflows.

4.1.7. *HH 731 and HH 1-100*

About 2′ west of HH 100 we detected two new HH knots, designated HH 731 A and B (see Fig. 4). HH 731A is a bright knot. HH 731B is a knot with faint [S II] emission extending to its southwest. Eight members of the Coronet cluster, IRS 1, 2, 5, 11–15 (Taylor & Storey 1984), and two emission-line stars, Hα 2/star 1-100 (Marraco & Rydgren 1981; Graham 1993) and CrA/1 (Walter 1986), are located within a radius of 2.′5 from HH 731A. IRS 1, 2, and 5 are Class I YSOs on the basis of their

spectral energy distributions (SEDs) (Wilking et al. 1986, 1992). IRS 2 and 5 are associated with MMS 9 and MMS 12, respectively (see Fig. 4). Without further information, such as proper motion, it is difficult to identify the exciting source of HH 731A and 731B in such a region clustered with young stars. However, given the properties of other HH outflow sources, the Class I sources, IRS 1, 2, and 5 are clearly the best candidates.

The HH object 1-100 HH was originally detected by Graham (1993). Our [S II] image shows that it consists of two condensations, 1-100 HH N and 1-100 HH S (see Fig. 4 and Fig. 8*c*). As for HH 731, its driving source cannot be reliably identified without further information, such as proper motion.

4.1.8. *HH 732*

HH 732 is located $\sim 4'$ to the east of TY CrA (Fig. 2). It consists of three parts, HH 732 A–C (Fig. 6). HH 732A is a knot that is somewhat elongated in the east-west direction. HH 732B is a faint knot, and 732C is a faint patch. HH 732A–C are apparently aligned.

HH 732 is located outside of the Coronet cluster. The nearest young star is TY CrA. However, the axis through the knots A–C does not point toward TY CrA. Therefore, a physical association with TY CrA is unlikely. There is no obvious other candidate for the exciting source along the axis defined by the knots A–C.

4.2. *Region around VV CrA*

Three new HH objects/HH object complexes are discovered in the VV CrA region (see Fig. 7). They have been given the numbers HH 861–863. HH 861 is located about $10'$ southwest of VV CrA. It consists of two emission patches, HH 861 A and B (Fig. 7*d*). HH 861A has an arclike shape facing southwest. HH 862 is a small patch located about $6'$ west of VV CrA and is elongated in the direction toward VV CrA (Fig. 7*c*). About $8'$ to the south and southeast of VV CrA, we detected five [S II] emission patches, designated HH 863 A–E. These emission patches are relatively large and diffuse.

One known young star, VV CrA, and four known millimeter sources, MMS 22–25 (Chini et al. 2003), are located in the VV CrA region. The strong millimeter source MMS 24 coincides well with the star VV CrA. VV CrA has long been known to show various spectroscopic signs of strong mass loss and is therefore a good candidate for an HH object source in this region. These spectroscopic signatures are P Cygni profiles in the Balmer lines (Hα, Hβ, and Hγ) and Na D lines, and strong and blueshifted [O I] $\lambda\lambda$6300, 6363 and [S II] $\lambda\lambda$6717, 6731 lines (e.g., Appenzeller et al. 1986; Hamann 1994). In the study by Mundt & Eislöffel (1998), a small sample of five T Tauri stars with spectroscopic signatures of strong mass loss similar to those of VV CrA, were searched for associated HH outflows. Indeed, around all of these five stars HH objects or HH jets are found, which indicates that T Tauri stars with strong forbidden lines and/or P Cygni profiles in the Balmer lines or Na D are potential HH object sources.

The star VV CrA has an infrared companion (separation $\sim 2''$; see Graham 1992). Koresko et al. (1997) found that the companion ($M \sim 2\ M_{\odot}$) is more massive than VV CrA itself ($M \sim 0.7\ M_{\odot}$). Since the companion is much more obscured than the optical primary, it is probably surrounded by more circumstellar material. Therefore, the infrared secondary may have a stronger accretion than VV CrA (Koresko et al. 1997). For this reason the companion is also a potential outflow source.

Recently, Takami et al. (2003) did spectroastrometric observations of the optical component of the VV CrA system in the highly blueshifted [O I] and [S II] lines. These blueshifted forbidden lines are highly extended toward P.A. $\sim 70^{\circ}$, as expected for a collimated outflow (see, e.g., Hirth et al. 1997). Quite interestingly, the P.A. of HH 861 with respect to VV CrA is just in the opposite direction, namely at $\sim 250^{\circ}$. Therefore, it is quite possible that HH 861 is driven by the redshifted outflow from the optical component of the VV CrA binary. If that is true, HH 861 should be redshifted. However, we do not find the expected blueshifted counterpart of HH 861 in our [S II] image, although we have conducted a careful search of HH emission in the direction of P.A. $\sim 70^{\circ}$. Maybe there is insufficient molecular cloud material with which the blueshifted part of the outflow can interact. We note that the morphology of HH 862 suggests that it may also be driven by VV CrA. In this case, the IR companion of VV CrA is the more likely source, since the optical component appears to excite HH 861.

The diffuse morphology of HH 863 A–E casts some doubt on their HH object nature for the following reason: in the high-contrast [S II] image displayed in Figure 7*a*, there is a small dark cloud visible about $3'$ south of VV CrA. This dark cloud is surrounded by a bright rim. Such bright rims are expected to be found around dark clouds because of the presence of a diffuse interstellar radiation field (in particular if the dark cloud is above the plane of the Milky Way, as is the case here). The UV part of this radiation field will also excite a thin ionization region ("H II region") at the dark cloud rim, which can be of relatively low ionization and therefore relatively strong in [S II] emission. For these reasons, it might be possible that HH 863 A–E represent just the brightest patches in this low-ionization region around this dark cloud. In principle, it cannot be totally excluded that HH 861 and HH 862 have the same physical nature, because they are also located in a region that shows patches of increased sky background due to dark cloud material. However, the much more compact structure of HH 861 and 862 does not favor this interpretation. Spectroscopic observations would clarify the situation.

5. GENERAL DISCUSSION

Our optical survey shows that abundant outflows exist in the R CrA molecular cloud. From the above discussion on individual HH objects, we identify at least five separate flows in the region around R CrA, namely the HH 82 and 729 flow, the HH 730, 860, 104D, and 99 flow, the HH 96, 97, 100, and 98 flow, the HH 733 flow, and the HH 734B flow (Fig. 5). In addition, a molecular outflow from IRS 7 at the orientation of P.A. $= 75^{\circ}$ was observed at millimeter wavelengths (Anderson et al. 1997). Therefore, at least six outflows can be identified in the R CrA region. These outflows indicate that the R CrA region is rather active in recent star formation.

Outflows from young stars may play an important role in injecting energy and momentum into the cloud. The numerous outflows observed in the R CrA region suggest that they could play a crucial role in the evolution of the R CrA cloud. A similar example was observed in the NGC 1333 region (Bally et al. 1996). However, the outflow activity reported here appears more intense than that observed in NGC 1333 in terms of outflow density. One dozen of the flows are observed in NGC 1333 within an area of 2 pc $\times$ 2 pc. In contrast, six flows are identified in R CrA within an area of 0.8 pc $\times$ 0.8 pc. Furthermore, if only the central 0.4 pc $\times$ 0.4 pc region around R CrA is considered, the derived outflow density is even higher.

In the VV CrA region, our survey also reveals three HH objects, HH 861–863, which indicates that active star formation is also going on in this region. These newly detected HH objects apparently represent three distinct outflows, with the

classical T Tauri star VV CrA being a candidate for driving HH 861. If some of the millimeter sources in the VV CrA region turn out to be the exciting source of the HH objects found there, then they are protostars rather than prestellar cores.

6. SUMMARY

A deep [S II] $\lambda\lambda$6717/6731 wide-field HH object survey was carried out in two fields toward the R CrA molecular cloud with a sky coverage of 0.62 deg^2. The main results of our survey are summarized as follows:

1. Twelve new HH objects, often consisting of several subcondensations, are discovered. These HH objects have the numbers HH 729–736 and 860–863. These much deeper optical data have been combined with the currently available optical, infrared, submillimeter, and millimeter wavelength observations to disentangle the various outflows present in this region.

2. At least five optical outflows in the R CrA and at least two in the VV CrA regions are identified on the basis of morphology, and the possible exciting sources of these outflows are discussed. HH 82 and 729 are driven by the T Tauri star S CrA. The giant flow consisting of HH 730, 860, 104D, and 99 is probably driven by the nebulous infrared source IRS 6. This flow extends over 12′ and has a spatial extent of 0.57 pc. HH 100-IRS apparently drives the outflow consisting of HH 96, 97, 100, and 98. HH 733 is probably driven by the T Tauri star T CrA. The HH 734B jet is likely to be driven by an NIR source of *K*-excess. The classical T Tauri star VV CrA, which shows various signs of strong mass loss, probably drives HH 861.

3. The detected outflows indicate that the R CrA region is rather active in recent star formation. The high density of outflows in the R CrA region also suggests that the outflows in this region could play an important role in the dynamics of molecular clouds and could therefore influence the current and future star formation rate of this region.

We would like to thank the ESO/MPG 2.2 m WFI group for making the observations in service mode. We thank Bo Reipurth for assigning official numbers to the newly detected HH objects reported in this paper and for his helpful comments. H. Wang acknowledges support by NSFC grants 10243004 and 10073021.

REFERENCES

Anderson, I. M., Harju, J., Knee, L. B. G., & Haikala, L. K. 1997, A&A, 321, 575
Appenzeller, I., Jetter, R., & Jankovics, I. 1986, A&AS, 64, 65
Appenzeller, I., Östreicher, R., & Jankovics, I. 1984, A&A, 141, 108
Appenzeller, I., & Wolf, B. 1977, A&A, 54, 713
Baade, M. 2002, Wide Field Imager (WFI) User's Manual (Garching: ESO), http://www.ls.eso.org/lasilla/Telescopes/2p2T/E2p2M/WFI/docs/manual/wfiuserman-1.0.7.ps
Bally, J., Devine, D., & Reipurth, B. 1996, ApJ, 473, L49
Brown, A. 1987, ApJ, 322, L31
Chini, R., et al. 2003, A&A, 409, 235
Choi, M., & Tatematsu, K. 2004, ApJ, 600, L55
Cohen, M., Harvey, P. M., Wilking, B. A., & Schwartz, R. D. 1984, ApJ, 281, 250
Davis, C. J., Smith, M. D., Eislöffel, J., & Davies, J. K. 1999, MNRAS, 308, 539
Eislöffel, J., & Mundt, R. 1998, AJ, 115, 1554
Eislöffel, J., Mundt, R., Ray, T. P., & Rodríguez, L. F. 2000, in Protostars and Planets IV, ed. V. Mannings, A. P. Boss, & S. S. Russell (Tucson: Univ. Arizona Press), 815
Gezari, D. Y., Pitts, P. S., & Schmitz, M. 1999, Catalog of Infrared Observations, Edition 5 (Strasbourg: CDS), http://vizier.cfa.harvard.edu/viz-bin/Cat?II/225
Ghez, A. M., McCarthy, D. W., Patience, J. L., & Beck, T. L. 1997, ApJ, 481, 378
Graham, J. A. 1992, PASP, 104, 479
———. 1993, PASP, 105, 561
Hamann, F. 1994, ApJS, 93, 485
Harju, J., Haikala, L. K., Mattila, K., Mauersberger, R., Booth, R. S., & Nordh, H. L. 1993, A&A, 278, 569
Hartigan, P., & Graham, J. A. 1987, AJ, 93, 913
Henning, Th., Launhardt, R., Steinacker, J., & Thamm, E. 1994, A&A, 291, 546
Herbig, G. H., & Bell, K. R. 1988, Third Catalog of Emission-Line Stars of the Orion Population (Lick Obs. Bull. 1111; Santa Cruz: Lick Obs.)
Hirth, G. A., Mundt, R., & Solf, J. 1997, A&AS, 126, 437
Joy, A. H., & van Biesbroeck, G. 1944, PASP, 56, 123
Knacke, R. F., Strom, K. M., Strom, S. E., Young, E., & Kunkel, W. 1973, ApJ, 179, 847
Knude, J., & Høg, E. 1998, A&A, 338, 897
Koresko, C. D., Herbst, T. M., & Leinert, Ch. 1997, ApJ, 480, 741
Loren, R. B. 1979, ApJ, 227, 832
Marraco, H. G., & Rydgren, A. E. 1981, AJ, 86, 62
Mundt, R. 1979, A&A, 74, 21
———. 1984, ApJ, 280, 749
Mundt, R., & Eislöffel, J. 1998, AJ, 116, 860
Neuhäuser, R., et al. 2000, A&AS, 146, 323
Reipurth, B., & Bally, J. 2001, ARA&A, 39, 403
Reipurth, B., Chini, R., Krügel, E., Kreysa, E., & Sievers, A. 1993, A&A, 273, 221
Reipurth, B., & Graham, J. A. 1988, A&A, 202, 219
Schwartz, R. D. 1978, ApJ, 223, 884
Schwartz, R. D., Jones, B. F., & Sirk, M. 1984, AJ, 89, 1735
Shu, F., Najita, J., Ostriker, E., Wilkin, F., Ruden, S., & Lizano, S. 1994, ApJ, 429, 781
Strom, S. E., Grasdalen, G. L., & Strom, K. M. 1974, ApJ, 191, 111
Suters, M., Stewart, R. T., Brown, A., & Zealey, W. 1996, AJ, 111, 320
Takami, M., Bailey, J., & Chrysostomou, A. 2003, A&A, 397, 675
Taylor, K. N. R., & Storey, J. W. V. 1984, MNRAS, 209, 5P
van den Ancker, M. E. 1999, Ph.D. thesis, Univ. Amsterdam
Walter, F. M. 1986, ApJ, 306, 573
Wilking, B. A., Greene, T. P., Lada, C. J., Meyer, M. R., & Young, E. T. 1992, ApJ, 397, 520
Wilking, B. A., McCaughrean, M. J., Burton, M. G., Giblin, T., Rayner, J. T., & Zinnecker, H. 1997, AJ, 114, 2029
Wilking, B. A., Taylor, K. N. R., & Storey, J. W. V. 1986, AJ, 92, 103
Yonekura, Y., Mizuno, N., Saito, H., Mizuno, A., Ogawa, H., & Fukui, Y. 1999, PASJ, 51, 911